JOURNAL OF GEOPHYSICAL RESEARCH, VOL. 112, C03S18, doi:10.1029/2006JC003726, 2007

Bora event variability and the role of air-sea feedback

Julie Pullen,[1] James D. Doyle,[1] Tracy Haack,[1] Clive Dorman,[2] Richard P. Signell,[3] and Craig M. Lee[4]

Received 23 May 2006; revised 22 September 2006; accepted 12 October 2006; published 13 February 2007.

[1] A two-way interacting high resolution numerical simulation of the Adriatic Sea using the Navy Coastal Ocean Model (NCOM) and Coupled Ocean/Atmosphere Mesoscale Prediction System (COAMPS®) was conducted to improve forecast momentum and heat flux fields, and to evaluate surface flux field differences for two consecutive bora events during February 2003. (COAMPS® is a registered trademark of the Naval Research Laboratory.) The strength, mean positions and extensions of the bora jets, and the atmospheric conditions driving them varied considerably between the two events. Bora 1 had 62% stronger heat flux and 51% larger momentum flux than bora 2. The latter displayed much greater diurnal variability characterized by inertial oscillations and the early morning strengthening of a west Adriatic barrier jet, beneath which a stronger west Adriatic ocean current developed. Elsewhere, surface ocean current differences between the two events were directly related to differences in wind stress curl generated by the position and strength of the individual bora jets. The mean heat flux bias was reduced by 72%, and heat flux RMSE reduced by 30% on average at four instrumented over-water sites in the two-way coupled simulation relative to the uncoupled control. Largest reductions in wind stress were found in the bora jets, while the biggest reductions in heat flux were found along the north and west coasts of the Adriatic. In bora 2, SST gradients impacted the wind stress curl along the north and west coasts, and in bora 1 wind stress curl was sensitive to the Istrian front position and strength. The two-way coupled simulation produced diminished surface current speeds of ∼12% over the northern Adriatic during both bora compared with a one-way coupled simulation.

Citation: Pullen, J., J. D. Doyle, T. Haack, C. Dorman, R. P. Signell, and C. M. Lee (2007), Bora event variability and the role of air-sea feedback, *J. Geophys. Res.*, *112*, C03S18, doi:10.1029/2006JC003726.

1. Introduction

[2] Numerous modeling and observational studies of the Adriatic Sea have emerged in the past several years. In particular, field programs such as the Mesoscale Alpine Programme (MAP, 1999), The Dynamics of Localized Currents and Eddy Variability in the Adriatic (DOLCEVITA), European Margin Strata Formation (EUROSTRATAFORM) and Adriatic Circulation, West Istria, and East Adriatic Coastal Experiments (ACE, WISE, EACE) (all 2002–2003) have motivated a fresh collection of synthesis studies of the Adriatic region [*Lee et al.*, 2005; *Sherwood et al.*, 2004]. The present research aims to explore and improve model deficiencies that have been uncovered during the scrutiny of model results in light of the recent 2002–2003 field campaigns. This work will also examine the atmospheric structure and oceanic response during two consecutive bora events in January–February 2003 that displayed contrasting characteristics.

[3] The downslope windstorms or "bora" that occur in the Dinaric Alps during the wintertime have been well-catalogued with respect to their synoptic settings. For instance, bora episodes have long been categorized as "cyclonic" (with a low situated over the Adriatic region and typically cloudy conditions) or "anticyclonic" (with a high pressure system sitting over northern Europe and commonly clear skies) based on the synoptic characteristics. Cyclonic bora usually possess stronger winds than anticyclonic bora. Additionally, the boundary layer depth during a bora may be shallow or deep, with anticyclonic bora often being deep and cyclonic bora tending to be shallow [*Defant*, 1951]. Bora can be combination cyclonic/anticyclonic or be driven by a frontal passage [*Jurcec*, 1988, 1989].

[4] It is only in the last several years that comprehensive studies involving aircraft flight data, in situ data, and high-resolution (<5 km) modeling have probed the mechanisms and variability of these intense wind events, thus developing a 3D picture of the atmospheric structure and its surface expression over the Adriatic Sea. Recently, as part of the 1999 MAP experiment, *Grubisic* [2004] identified the bora jets as terrain-locked features. The Trieste and Senj jets are

[1]Marine Meteorology Division, Naval Research Laboratory, Monterey, California, USA.
[2]Scripps Institution of Oceanography, University of California, San Diego, La Jolla, California, USA.
[3]U.S. Geological Survey, Woods Hole, Massachusetts, USA.
[4]Applied Physics Laboratory, University of Washington, Seattle, Washington, USA.

0148-0227/07/2006JC003726$09.00

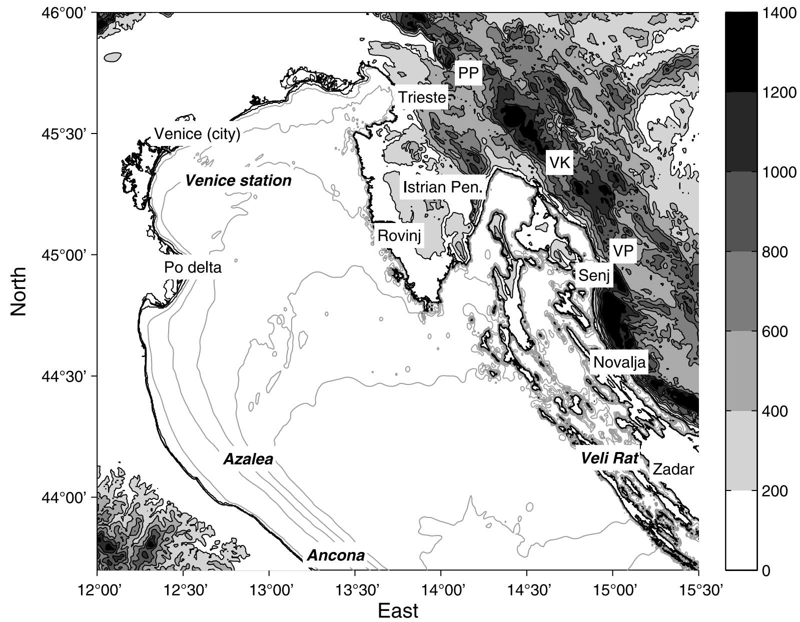

Figure 1. Depiction of the northern Adriatic with major topographic features and locations mentioned in the text labeled. Topography (m) is shaded, and bathymetry is contoured (in light grey) at the 10, 20, 30, 40, 50, 75, and 100 m levels. PP, Postojna Pass; VK, Velika Kapela; VP, Vratnik Pass. Over-water stations used in the model evaluation of section 7 are labeled in bold italics.

positioned downstream of the Postojna and Vratnik/Velika Kapela passes (mountain gaps), respectively, which allows the jets to interact with the surface and accelerate over the sea (Figure 1). To the south there are also jets at Novalja and Sibenik. By contrast, "wake" regions form downstream of high orography, where strong gravity wave breaking inhibits the extension of organized winds down to the surface. The wakes are interspersed between the jets, with the latter typically having a width of 25 km.

[5] *Gohm and Mayr* [2005] present a detailed study of a March 2002 anticyclonic deep bora that was relatively weak and lacked a surface expression of the Trieste jet. Aircraft measurements (lidar backscatter) as well as surface stations and soundings in the vicinity of the Senj jet were well-reproduced by the subkilometer resolution model simulation. Their analyses contribute to the understanding of the bora dynamics and processes. In their modeling studies, flow detaches from the lee side of steep terrain, stays aloft in the wake regions, but reattaches to the surface about 10–15 km offshore in the jets. This process is attributable to a combination of an adverse pressure gradient beneath the gravity wave and friction effects since the boundary layer separation did not occur in their frictionless (free-slip) sensitivity run. Moreover, their work identified the nocturnal intensification and daytime weakening of gravity wave amplitudes (and hence downslope wind speeds) as a result of the convective mixed layer development in the daytime. Finally, their high-resolution simulation distinguished two narrow jets that flow together to form the Senj jet.

[6] *Jiang and Doyle* [2005] examined the dynamical characteristics of bora winds. In their consideration of a November 1999 strong cyclonic bora using 1-km resolution COAMPS simulations along with aircraft observations, they show stronger wave breaking (and more dissipation) downstream of mountain peaks with a thin layer of fast supercritical flow conducive to boundary layer hydraulic jumps that minimizes the surface flow in the wake regions. This contrasts with weaker wave breaking downstream of mountain gaps with a deep layer of fast but less supercritical flow that favors extension of the high speed flow out over the sea in jets.

[7] Much attention has been directed at documenting and probing the double gyre current pattern that dominates the northern Adriatic Sea in response to the bora jets. Localized current meter measurements off the Istrian Peninsula suggested the double gyre system occurred as a response to the positive curl offshore of the region north of Rovinj on the Istrian Peninsula, and negative curl south of that point [*Zore-Armanda and Gacic*, 1987]. *Orlic et al.* [1994] originally conducted idealized modeling experiments of the double gyre using wind forcing based on this simple conception of the bora wind stress curl field. *Paklar et al.* [2001] simulated at high resolution the response of the ocean to one realistic short bora event. Their simulation included a double gyre circulation, but it was not the focus of their study.

[8] In idealized 2D modeling studies, *Enger and Grisogono* [1998] found that a spatially uniform warmer SST promoted extension of the bora farther out over the open sea than did a spatially uniform cooler SST, because the buoyancy flux sustained the supercritical flow in the bora mountain wave. However, the warmer SST had no impact on the maximum wind speed attained in the bora. Later, *Paklar et al.* [2005] conducted numerical experiments of winds containing an idealized bora structure, but with enhanced or decreased magnitude and extension across the basin in order to investigate the resultant ocean currents. They related the extension and strength of observed bora to the synoptic structure, with

anticyclonic bora being associated with rapid offshore decay and weak winds and cyclonic bora being linked to offshore extension and strong winds. Offshore extension appeared to be the primary controlling factor for the appearance of the ocean double gyre. In simulations of fast offshore decay (independent of wind speed) the anticyclonic ocean gyre did not appear.

[9] Since 2000, output from the triply nested (36, 12, 4 km) COAMPS atmospheric model reanalysis (termed the "control" run in this paper) has been distributed within the Adriatic oceanographic research community in anticipation of the intensive observational field programs of 2002–2003. Investigators have begun to compare the model fields with observations and to utilize the model fields in the interpretation of observations. The atmospheric model fields have also been used to force multiple ocean models. The COAMPS model fields cover the time period 1999–2003.

[10] *Pullen et al.* [2003] used the COAMPS 4-km atmospheric reanalyses to force the Navy Coastal Ocean Model (NCOM) configured for the whole Adriatic at 2-km resolution. In realistic simulations of winter and spring 2001 they applied EOF statistical analysis to describe the ocean double gyre as a generic response to bora forcing. Furthermore, they determined that the 4-km resolution nest produced superior winds to the 36-km resolution (outer) nest as well as reproducing the expected well-defined bora jet structure. In addition, the 4-km forcing fields generated more skillful ocean current predictions than did the 36-km fields when compared with Acoustic Doppler Current Profiler (ADCP) observations.

[11] Recently, *Kuzmic et al.* [2006] investigated the double gyre pattern using in situ ADCP data and high-resolution modeling for January–February 2003. In the ocean, the northern cyclonic "Trieste" gyre was found to be highly polarized with stronger and more barotropic flow over the shallow bathymetry on the northwest side and weaker more depth-dependent flow over deeper bathymetry on the east/northeast side of the gyre. The "Rovinj" anticyclonic gyre, by contrast, was circular in shape and barotropic in nature. Their ocean models (NCOM and a finite element model) were forced by the COAMPS 4-km surface fluxes, and *Kuzmic et al.* [2006] noted a tendency for the COAMPS wind stress to be too strong on the eastern side of the Adriatic at the Senj and Trieste surface stations during bora events. In addition, NCOM-generated surface currents were too strong during bora events when compared with velocities measured by several ADCP in the Trieste and Rovinj gyres.

[12] In work explicitly focused on atmospheric observations on or near the water, *Dorman et al.* [2006] collected wind stress and heat flux data at several gas platforms and coastal land-based stations in the northern Adriatic during January–February 2003. They found elevated heat loss on the northeastern side of the Adriatic with minimal heat loss occurring in the midnorthwestern portion. The 4-km resolution COAMPS reanalysis overpredicted the heat fluxes in the northern Adriatic. In addition, COAMPS wind stress values were often too large. For example, at Veli Rat, near the Senj jet on the east coast of the Adriatic, the COAMPS wind stress was twice as large as the observed values during February.

[13] The suggestion that the COAMPS surface fluxes were too strong in January–February 2003 motivated the current work focused on examining and improving the momentum and heat flux model predictions by incorporating two-way coupling between COAMPS and an ocean model. Recently, *Pullen et al.* [2006] used the Adriatic ocean and atmosphere model configurations from *Pullen et al.* [2003] and included two-way coupling between the models by supplying COAMPS with 6-hourly SSTs produced by the ocean model (NCOM) in response to the COAMPS forcing. In simulations of fall 2002, they demonstrated increased skill in wind speed forecasts in the northern Adriatic at three over-water platforms and one land-based station using two-way coupling. In particular, winds produced by the two-way coupled simulation were slower and accorded better with observations than the control winds. Building on these results, we extend the simulations to winter 2003, which included several strong bora events. This gives us an opportunity to evaluate control, one-way coupled (uses control momentum fluxes but recalculates heat fluxes using ocean model SST) and two-way coupled heat fluxes and wind stresses in the context of the intensive observational campaign, and to compare and contrast two distinct bora events and examine their effect on the ocean.

[14] The model configuration is reviewed in section 2, followed by an overview of two modeled bora events in winter 2003 in section 3 and an assessment of the differences between the fields produced by the control and two-way coupled COAMPS in section 4. Section 5 focuses on the differential ocean response to the two bora events and the representation of the ocean currents within the one-way and two-way coupled models. The role of bulk flux parameterizations in modulating and improving atmospheric fluxes when used to force the ocean model in one-way coupling is explored in section 6. Section 7 compares measured wind stress and heat fluxes with modeled quantities. Section 8 contains the discussion and conclusions.

2. Model Configuration

[15] The model setup has previously been described in detail by *Pullen et al.* [2003] (control and one-way coupled) and *Pullen et al.* [2006] (two-way coupled). Key aspects of the model configuration will be reviewed here. COAMPS is a nonhydrostatic model with full physics parameterizations and an MVOI data-assimilation system [*Hodur*, 1997; *Chen et al.*, 2003]. It employs the Louis surface flux parameterization [*Louis et al.*, 1981]. The COAMPS Adriatic configuration is a triply nested (36, 12, 4 km) domain where nest 3 extends from 39.6°N to 47.3°N and 10.4°E to 20.6°E with horizontal dimensions of 187 $\times$ 205. There are 30 vertical terrain-following levels. At 00 UTC and 12 UTC of each day a data assimilation cycle is initiated using the prior 12-h forecast as background, and incorporating quality-controlled observations from aircraft, radiosondes, satellite, ship, and surface stations. An optimum interpolation (OI) analysis utilizing satellite and in situ SST measurements is also conducted at these times and the SST field is held fixed over the subsequent forecast cycle lasting 15 hours. The simulation has been run continuously in this mode for the time period September 1999 through June 2003. This simulation is referred to as the control run, and the resultant surface fluxes have been used to drive various ocean models

[*Pullen et al.*, 2003, 2006; *Kuzmic et al.*, 2006; *Martin et al.*, 2006].

[16] The ocean model NCOM [*Martin*, 2000] was configured for a region covering the entire Adriatic with 2-km horizontal resolution and 50 vertical levels (36 of which are sigma coordinates in the upper 190 m of the water column). NCOM is initialized using temperature and salinity fields from a 12 UTC 19 January 2003 ROMS simulation that was forced with COAMPS control run fluxes modified using the COARE 3.0 bulk algorithm (R. P. Signell et al., manuscript in preparation, 2006). Then a five-day diagnostic spin-up is run using wind fields from the previous five days while holding temperature and salinity fixed in order to permit adjustment of the velocity field. This is followed by a six-day prognostic run to 12 UTC 25 January 2003. The simulation is then advanced forward from this state in both the one-way and two-way coupled mode. Although a full 3D MVOI ocean data assimilation system is linked to NCOM, this capability is turned off in the runs described here due to a lack of telemetered, quality-controlled observations at fine scales in the simulation domain and also in order to simplify the interpretation of the model results. River discharge from 22 sources within the Adriatic is introduced as forcing in the simulation. Where available, hourly data from river gauges are used. Otherwise, monthly climatological values based on *Raicich* [1994] are inserted.

[17] In the one-way coupled run shown in section 5, the COAMPS control hourly momentum fluxes (using model forecast hours 1 to 12) are applied directly, but as in *Pullen et al.* [2003], *Kuzmic et al.* [2006], and *Martin et al.* [2006] hourly heat fluxes are computed using *Kondo* [1975] neutral drag coefficients and the ocean model SST. The heat fluxes computed in this manner are referred to as the one-way coupled results and are saved and examined in section 6.

[18] In the two-way coupled simulation, the COAMPS data assimilation cycle is still 12 hours, but SST fields from the NCOM ocean model are fed back at a 6-hour interval to the COAMPS 4-km nest [*Pullen et al.*, 2006]. COAMPS hourly momentum and heat fluxes are used to directly force NCOM in the two-way coupled simulation. In the two-way coupling, a modified Louis surface flux scheme is used [*Wang et al.*, 2002]. This scheme has been demonstrated to reduce surface heat fluxes by approximately 10–20% within the bora jets compared with the original Louis scheme used in the control run, and is in better agreement with flux observations in coastal regions (Wang, personal communication). The inclusion of the modified Louis flux scheme makes a direct comparison with the one-way coupled simulation more complex. However, the improved flux scheme was applied in the two-way coupled experiment in order to produce the most accurate fluxes possible.

3. Bora Event Variability

[19] There is some degree of subjectivity in bora event identification. *Kuzmic et al.* [2006] define bora as northeasterly wind events at Senj exceeding 5 m s^{-1}, lasting 3 days, and being representative of flow at Trieste as well. They selected 9–14 February 2003 as a bora time period. *Lee et al.* [2005] use a slightly different definition of a bora and note that there was one long bora event 11–19 February 2003. *Dorman et al.* [2006] describe a bora as northeasterly winds at Zadar greater than 2.6 m s^{-1} lasting at least 24 hours. They chose a lower threshold speed as Zadar feels the influence of bora-oriented winds but is not situated within a bora jet. This latter definition of bora events proved useful in the analyses presented by *Dorman et al.* [2006]. We retain that definition here and focus on two bora from 1400 UTC 31 January to 0600 UTC 2 February 2003 (41 hours) hereafter termed "bora 1" and 0700 UTC 11 February to 0400 UTC 14 February 2003 (70 hours) called "bora 2" in the subsequent discussion. These two consecutive bora have contrasting features that illustrate the variability expressed by different bora.

[20] The sea level pressure during bora 1 consists of a low pressure cell in the Mediterranean Sea to the south of Sardinia, creating a favorable pressure gradient for bora formation over the northern Adriatic (Figure 2a). At upper levels, a cutoff low is evident in the same position within a trough over north central Eurasia (Figure 2b). This creates a robust reverse flow aloft over the northern Adriatic that is maintained at subsequent times (Figure 2c). Reversed upper level flow is associated with strong bora and other downslope wind storms [*Jurcec*, 1989; *Grubisic*, 2004; *Smith*, 1987]. The synoptic setting of bora 1 suggests a cyclonic bora.

[21] In bora 2 the orientation and strength of the pressure gradient is initially similar to bora 1. What differentiates them is the subsequent reorientation of the sea level pressure gradient throughout bora 2 as well as a lack of reversed upper level flow. At the surface during bora 2 an anticyclone is situated over north central Europe so the sea level pressure gradient aligns northeast to southwest across the northern Adriatic, which is consistent with bora flow (Figure 2d). After 36 hours has elapsed, a shift in the position of the anticyclone orients the sea level pressure gradient from southeast to northwest, thereby inducing a variation in the bora direction (Figure 2e). Aloft, the 500 hPa geopotential height field contains a low over the Adriatic, which generates upper level bora-oriented flow (Figure 2f). Upper level flow in the same direction as the lower level is often a feature of weak bora [*Jurcec*, 1989; *Gohm and Mayr*, 2005]. The synoptic environment of bora 2 is reminiscent of an anticyclonic bora.

[22] Bora 1 and 2 are differentiated further by their mean potential temperature along a cross-section through the Senj jet in the two-way coupled simulation (Figure 3, with cross-section location shown in Figures 4a and 4d). In both bora, a jet of cold air streams across the Adriatic. In bora 1 the jet extends farther across the basin and the air is warmer in comparison with bora 2. During bora 1 there is a well-defined boundary layer over the Adriatic approximately 650 m deep; whereas the atmosphere is more uniformly stably stratified up to a height of 1000 m in bora 2. Bora 2 also has a pronounced patch of cold air along the west coast of the Adriatic overlying the adjacent Appenine mountains. This cold air, in concert with the blocking created by the mountain range, deflects the oncoming bora flow. These factors create a pressure gradient effect that generates a diurnally varying barrier jet during bora 2, leading to northwesterly coastal flow on the Adriatic's west side with a surface expression that was documented by F. Askari et al. (SAR mapping of northern Adriatic bora winds, submitted to *Journal of Geophysical Research*, 2007, hereinafter referred to as Askari et al., submitted manuscript, 2007) and will be explored at the end of this section.

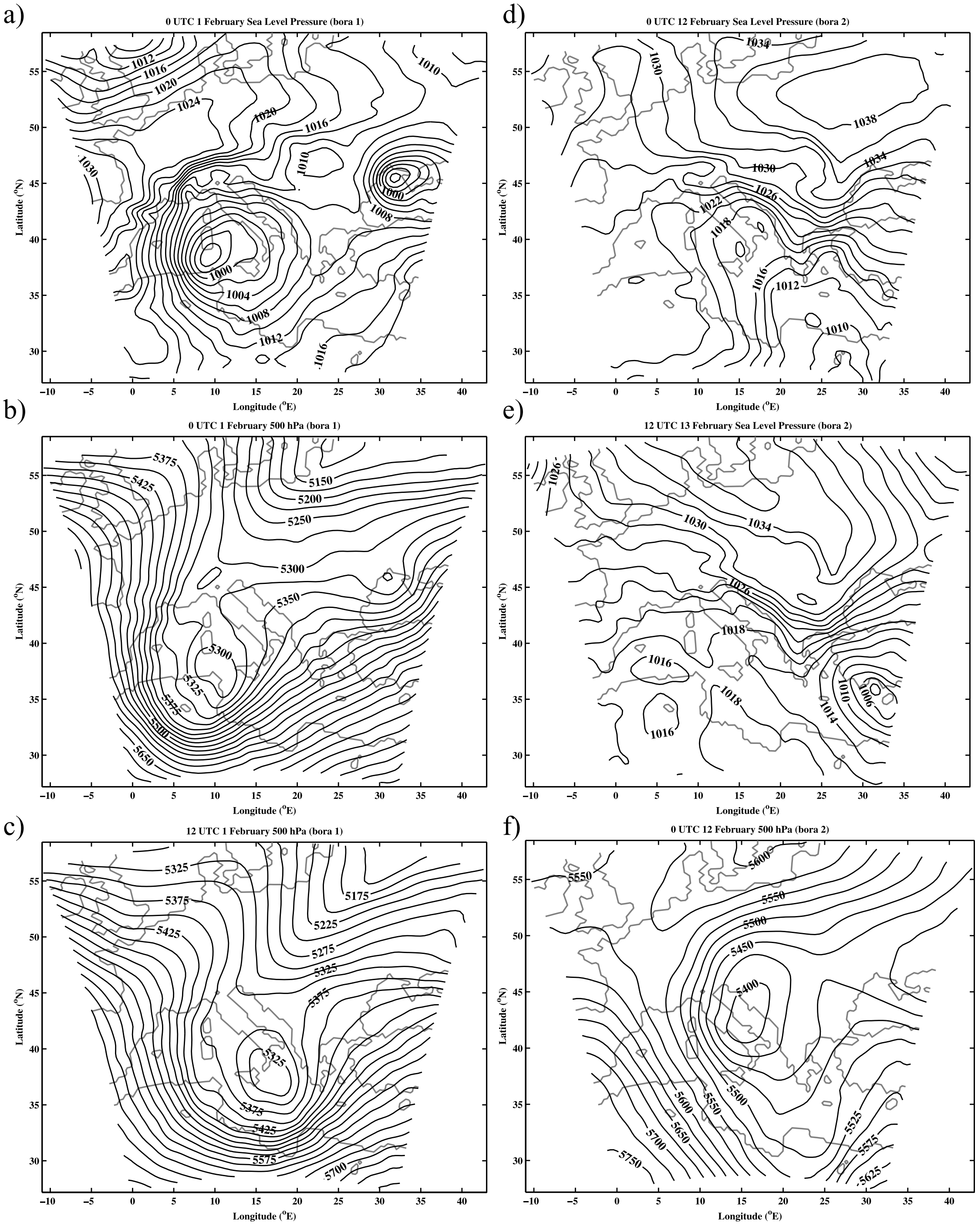

Figure 2. Snapshots of sea level pressure and 500 hPa geopotential height during (left) bora 1 and (right) bora 2 from the outermost nest (36 km) COAMPS analysis. Sea level pressure is in millibars, and geopotential height is in meters.

[23] In the two-way coupled simulation, during bora 1 the jets extend farther across the basin and the wind stress is stronger than in bora 2 (Figures 4b and 4e). Other differences relate to the Trieste jet. In bora 2 the Trieste jet is stronger than in bora 1 as it leaves the coast and encounters the water, and the position of the Trieste bora jet is displaced northward in bora 2 relative to bora 1. Additionally, the jet at Sibenik (the southernmost jet in the domain) is virtually absent in bora 2, although it has a strong signature in bora 1. Finally, the wind stress in bora 1 is more temporally variable than in bora 2 (standard deviation plots not shown). This variability is due to the gradual increase followed by a decrease of the maximum bora wind speeds that occurred around 0900 UTC 1 February 2003. These features of the wind stress field are consistent with those described by *Dorman et al.* [2006] using the control run model output.

[24] The distinctions in the jet structure between bora 1 and bora 2 are further reflected in the two-way coupled

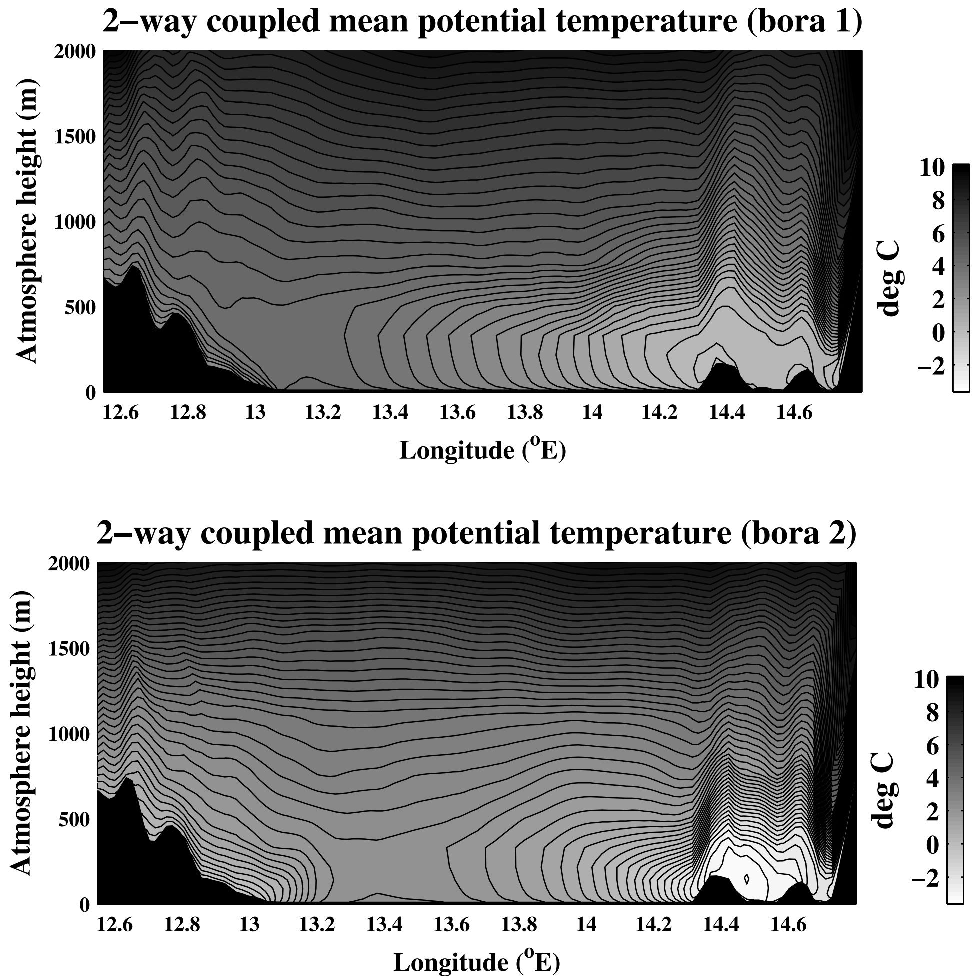

Figure 3. Mean two-way coupled potential temperature for bora 1 and bora 2 through the Senj jet transect shown in Figures 4a and 4d. Terrain is shaded in black.

wind stress curl field (Figures 4c and 4f). The mean wind stress curl field during bora 1 contains bands of alternating sign extending across the basin. By contrast, the mean wind stress curl during bora 2 is more diffuse in nature; for instance, there is a broad region of negative curl off the Istrian Peninsula in bora 2 that is resolved into two differentiated bands of negative curl during bora 1. In bora 1, mean negative curl dominates the northern Adriatic in the Gulf of Trieste, but negative curl is pressed against the northern boundary in bora 2. The wind stress curl field of bora 2 is reminiscent of the idealized bora vorticity pattern of *Zore-Armanda and Gacic* [1987] and *Orlic et al.* [1994]; however, the reduction of wind stress in the northern Gulf of Trieste and concomitant negative wind stress curl against the northern coast was not included in their schematic representation of the wind field. The ocean circulation is expected to be sensitive to the differences in wind stress curl displayed by the two bora events. This topic will be addressed in section 5.

[25] Differences between bora 1 and bora 2 are also evident in the two-way coupled mean total heat flux (Figures 4a and 4d), including the distinctions between the Trieste jet as represented in bora 1 and bora 2 and the extension of large upward heat fluxes across the basin in bora 1. The mean total heat flux over the domain shown is 453 W m^{-2} in bora 1 and 283 W m^{-2} in bora 2. Whereas wind stress variability is highest during bora 1, heat flux variability is greater in bora 2 in all the jets except the Trieste jet (standard deviation plots not shown), indicative of a greater impact of diurnal forcing in bora 2.

[26] The shift in the gradient of the sea level pressure in bora 2 (shown in Figures 2d and 2e) is responsible for variations in the position of the Senj and Trieste jets over time (Figures 5a and 5b). This contributes to the mean surface fields being weaker in bora 2 relative to bora 1. Bora 2, being a weaker event, is more susceptible to local mesoscale effects. Apart from adjustments of the large scale pressure gradient alignment, there is meandering on a shorter timescale (inertial) that corresponds to the diurnal pressure gradient interacting with frictional drag. The pulsating characteristics of bora 2 are consistent with an inertial oscillation: the inertial period for this latitude is 17 hours. Winds are rotated toward low pressure at 15 UTC and toward high pressure 18 hours later at 9 UTC with a maximum speed occurring in between these two times at 21 UTC, about 5 hours after sunset (~1630 UTC in February). These winds are about 2 m s^{-1} greater than the geostrophic wind speed of 15 m s^{-1} and are consistent with the inertially driven increase in the nocturnal jet reported by *Garratt* [1985] and *Kraus et al.* [1985].

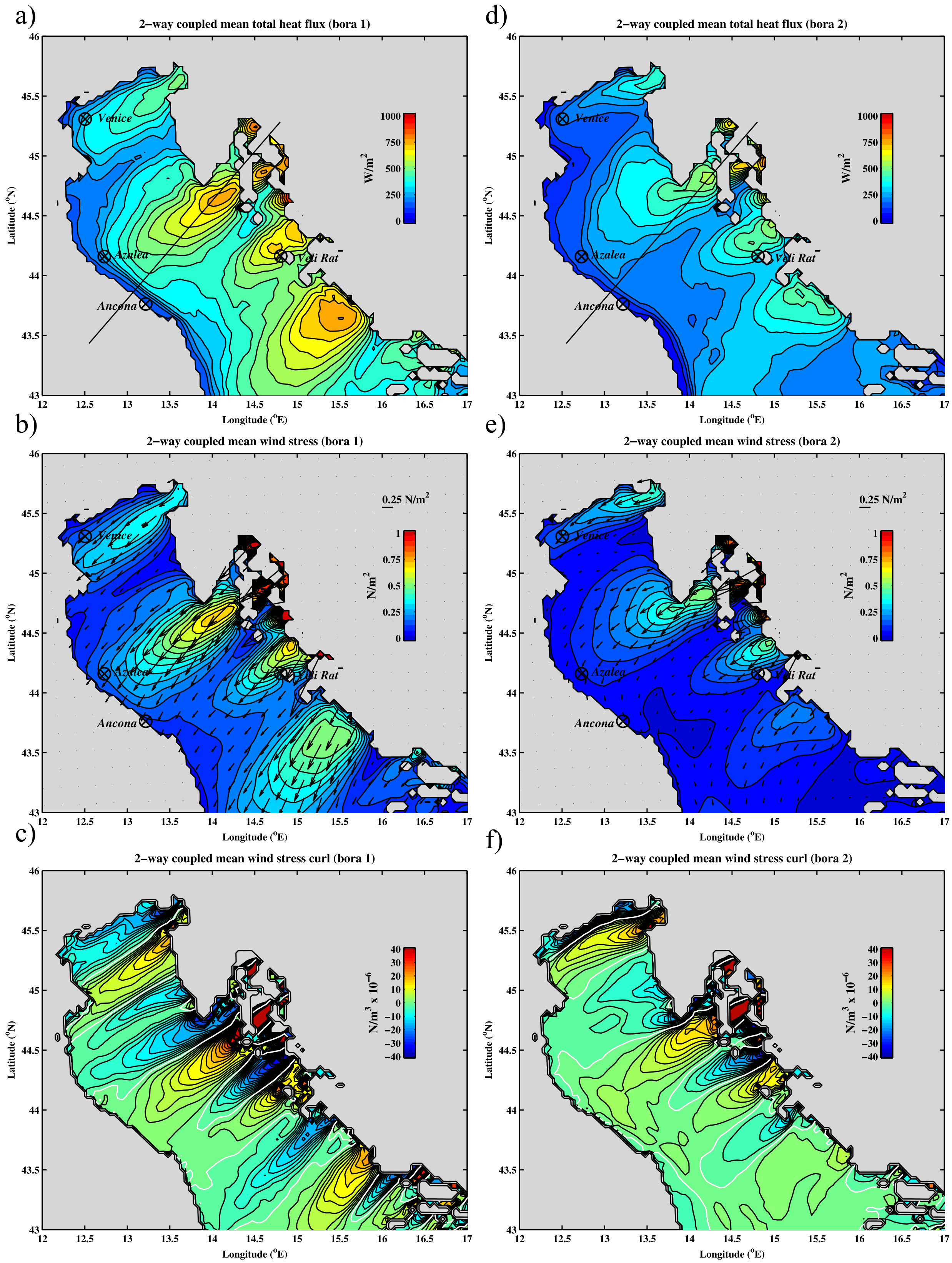

Figure 4. Mean two-way coupled surface flux fields and wind stress curl for bora 1 and bora 2.

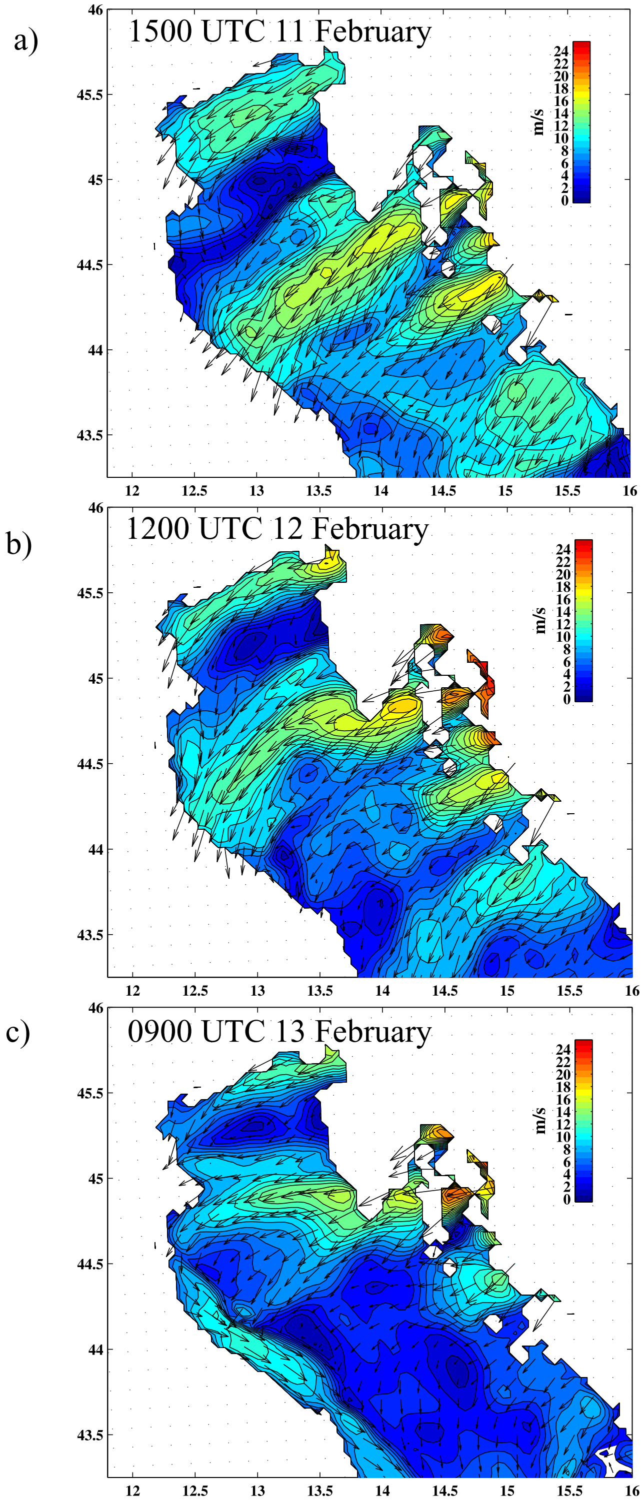

Figure 5. Snapshots of bora 2 10-m wind evolution at 21 hour intervals.

[27] Bora 2 is also affected by barrier jet evolution. The barrier jet whose generating mechanism was suggested by Figure 3b has a surface expression of northwesterly atmospheric flow adjacent to the west coast of the Adriatic (Figure 5c). Synthetic Aperture Radar images shown by Askari et al. (submitted manuscript, 2007) from January to February 2003 show the barrier jet to be a common feature in the surface wind field. It occurs intermittently throughout bora 2 and serves to truncate the extension of the Senj jet across the basin in the mean. Also, the barrier jet tends to occur in the early morning hours of bora 2 due to the differential cooling over land relative to the ocean that contributes to the dynamics of the jet and that is eroded in the daytime. So the barrier jet is another feature that contains a diurnal signature that has an important impact on the surface fields in bora 2.

4. Impact of Air-Sea Coupling on Bora Events

[28] Now we turn to an assessment of the two-way coupled simulation for bora 1 and bora 2, with reference to the control run. The main differences in the fields between the control and two-way coupled runs are attributable to differences in SST. During bora 1, the control SST (which uses an analyzed OI SST product) presents a relatively smooth north/south SST gradient with approximately 4°C temperature increase to the south (Figure 6a), a significantly smaller range than observed (Figure 6c). In contrast, the two-way coupled run (Figure 6b) produces broad 10°C north-to-south SST differences that match those observed in contemporaneous satellite-derived SST and in situ measurements (Figure 6c). The two-way coupled run exhibits striking small-scale structure, such as the narrow band of cold water along the shallow northern and western boundaries that mirrors the observed SST and is responsible for the increased north-to-south gradient in the two-way coupled simulation. The two-way coupled run also features an intense SST front at the southern tip of the Istrian Peninsula and a warm, "shingled" filament extending from the strongly sheared region to the west.

[29] In bora 2, temperatures generally decrease by approximately 2°C, with more dramatic cooling along the northern and western Adriatic (not shown). Otherwise the general pattern of modeled SST remains the same. High-resolution (0.25 km) surveys conducted using a towed profiling vehicle (SeaSoar) sampled the Istrian front and Po plume extension during bora 2. SeaSoar sections across the Istrian front revealed temperature changes of approximately 3°C over distances of less than 1 km, with salinity compensating the small density contrast that existed across the front [*Peters et al.*, 2006]. During periods of strong forcing, the water column remained unstratified and sea surface properties near the front extended to the seabed. As the forcing weakened, frontal gradients began to tilt, introducing weak stratification. The two-way coupled model produces an Istrian front that is consistent in location, scale and strength with the observations. *Zore-Armanda and Gacic* [1987] associate front formation and position with the frequency and intensity of bora events, with strong easterly bora along the Senj pathway producing zonal alignment while weak forcing produces meridional orientation. The improved characterization of winds and surface fluxes provided by the two-way coupled model may be a critical element governing its ability to simulate the small-scale features that dominate northern Adriatic response to bora.

[30] Mean heat fluxes during bora 1 are reduced in the two-way coupled simulation (Figure 7a). Over the domain shown this amounts to an average reduction of 133 W m^{-2}

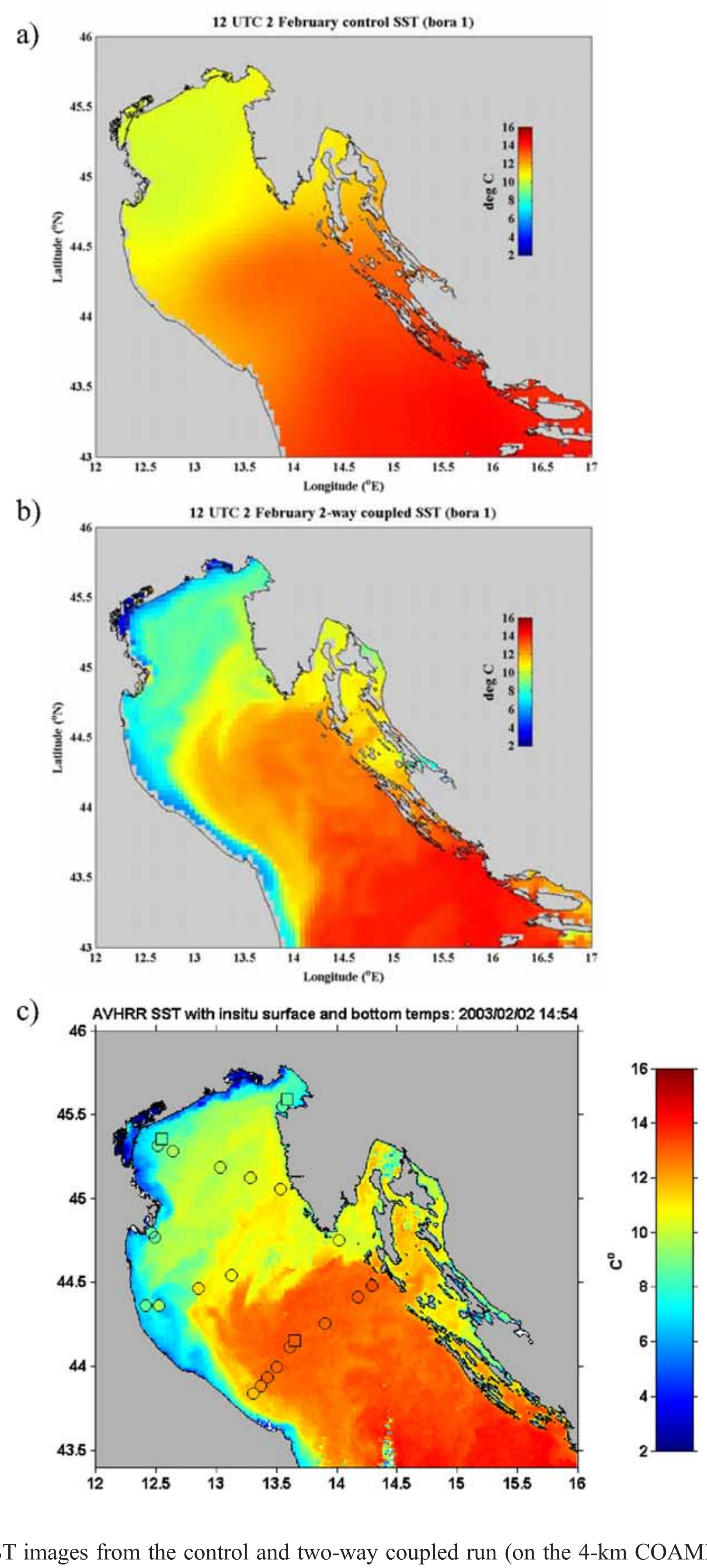

Figure 6. SST images from the control and two-way coupled run (on the 4-km COAMPS grid) along with AVHRR SST with in situ surface (bottom) measurements colored with a solid circle (square).

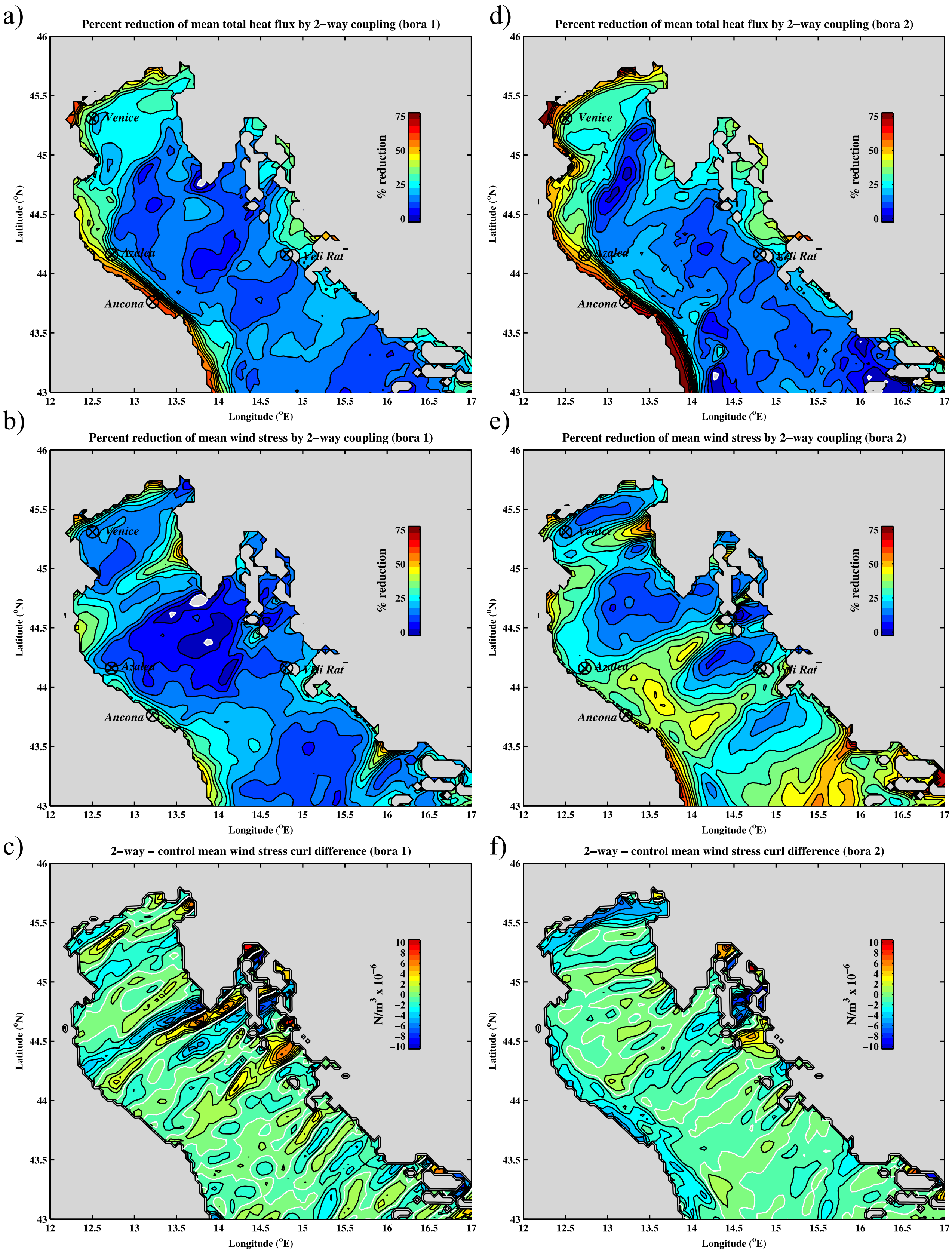

Figure 7. Percent reduction of wind stress and total heat flux, and wind stress curl difference, for bora 1 and bora 2.

relative to the control run, with reductions of over 200 W m^{-2} in the bora jets and on the northern and western fringes of the Adriatic. As a percentage of the control simulation heat fluxes, this represents a 23% average decrease over the whole domain, with over 25% reduction inshore of Veli Rat and in the Gulf of Trieste and over 50% reduction along the west coast. There is also a decrease in heat flux variability during bora 1 using the two-way coupled simulation by 27 W m^{-2} on average over the domain and locally over 50 W m^{-2} in regions next to the coast where bora jets are situated (not shown).

[31] The magnitude of the mean wind stress in the bora jets is diminished in the two-way coupled simulation compared with the control run in bora 1, especially in the Trieste jet. In terms of an average over the domain, the reduction amounts to 0.0581 N m^{-2} relative to the control simulation. Locally, however, the largest percentage reduction of wind stress, relative to the control, occurs in the bora wake regions, along the northern side of the Adriatic, and off the Istrian Peninsula (Figure 7b). There is also diminished wind stress by up to 50% along the western Adriatic in the two-way coupled simulation. Wind stress curl fields are overall weaker in the two-way coupled simulation. The wind stress curl difference fields show a strong imprint of the Istrian front in bora 1 (Figure 7c) as does the wind stress standard deviation (not shown).

[32] During bora 2, the heat flux mean difference (two-way coupled minus control) over the domain is 102 W m^{-2}, which is a weaker reduction (by 31 W m^{-2}) than was found during bora 1. However, in percent terms the total heat flux over the northern Adriatic is reduced by 26%, which is comparable to the percent reduction during bora 1 (Figure 7d). Localized regions in the north and west experience a significantly larger drop in heat flux (over 75% in some places) in the two-way coupled run. As in bora 1, heat flux variability is reduced in the two-way coupled simulation, but by only 12 W m^{-2} overall (compared to 27 W m^{-2} in bora 1) (not shown).

[33] The domain-averaged two-way coupled wind stress field difference from the control run is 0.0512 N m^{-2} in bora 2 (and thus slightly smaller than for bora 1), with largest absolute reductions in the jets, especially for the Trieste jet. The percent reduction is higher overall compared with bora 1, with predominantly wake regions being reduced in wind stress magnitude by approximately 50% (Figure 7e).

[34] The wind stress curl field in the two-way coupled simulation has more negative curl near the northern edge of the Adriatic, and reduced positive curl over the rest of the Gulf of Trieste (Figure 7f). There is reduced positive curl in the Senj jet and more negative curl along the west side in the two-way coupled run compared with the control run.

[35] To review the differences between the control and two-way coupled runs: the greatest absolute reduction in heat flux and wind stress occurs during bora 1 (133 W m^{-2} and 0.0581 N m^{-2}), the stronger bora. During both bora the largest differences in heat flux are along the north and west fringes due to the dramatically colder SSTs in the two-way coupled simulation. In the bora jets, large differences in heat flux occur along with the greatest differences in wind stress. The reduced heat fluxes and wind stress in the bora jets are attributable to the relatively cooler SSTs in the two-way coupled simulation [*Pullen et al.*, 2006], especially below the Trieste jet (Figure 6). In bora 1, the wind stress standard deviation and curl show strong sensitivity to the location of the Istrian front (broad and diffuse SSTs in the control run and tight and confined SSTs in the two-way coupled run, as seen in Figure 6).

[36] The more negative curl in the Trieste jet in bora 2 for the two-way coupled simulation relative to the control run is likely linked to the underlying cold SSTs along the north side of the Adriatic. Using satellite fields, *Chelton et al.* [2004] correlated wind stress curl with cross-wind SST gradient over portions of the global ocean; for example, winds blowing east–west with cold water to the north induces negative curl. In the Gulf of Trieste, the winds blow parallel to the isotherms (a cross-wind SST gradient) during bora 2 because the Trieste jet is positioned up against the coastline. So an SST impact on the curl field is to be expected, particularly due to the location of the Trieste jet during bora 2. Also, in the two-way coupled simulation, the high percentage reduction of wind stress and absolute reduction of wind stress curl on the western side of the Adriatic in bora 2 is presumably due to the barrier jet flowing over cold water and leading to reduced winds there. The cold SSTs are not represented in the control simulation so this effect would be missing in those fields. The physical mechanisms of the coupled response are explored in more detail by *Pullen et al.* [2006].

5. Bora Effect on Ocean Currents

[37] As was shown in section 3, the wind stress and heat flux patterns differed between the two bora events in February 2003. In particular, the wind stress curl field of bora 1 was more banded along the axis of the basin, while the bora 2 field was more diffuse. The refined wind stress curl pattern given by the high-resolution COAMPS, and especially the two-way coupled run, affords an assessment of interbora (bora 1 versus bora 2) and intrabora (one-way versus two-way) differences in ocean surface currents.

[38] The two-way coupled interbora differences in ocean surface currents are most pronounced beneath the bora jets and in the western Adriatic (Figure 8). In contrast to the idealized simulation results of *Paklar et al.* [2005], despite the offshore extent of the bora jets being substantially reduced in bora 2 relative to bora 1, the simulated ocean still produced the double gyre circulation during bora 2. Under the Trieste jet the northern arm of the Trieste gyre is weaker and displaced farther south in bora 1 compared with bora 2. Likewise, the anticyclonic Rovinj gyre is located farther south during bora 1 compared with bora 2. This is a direct response to the wind stress curl field produced by the different positions of the Trieste bora jet during bora 1 and 2 (Figures 4a, 4d, 4c, and 4f). The ocean flow is strong under the Senj jet in both bora, but the bora 1 current is broader, swifter, and located farther south of the Istrian tip relative to the flow in bora 2. The position of the ocean current is again a function of the differing location of the Senj jet between the bora.

[39] Along the western Adriatic coast there is a stronger West Adriatic Current (WAC) during bora 2, which is not related to Po river runoff, as discharge rates were declining between bora 1 and bora 2 and were quite weak ($\sim$1000 m^3 s^{-1}) compared

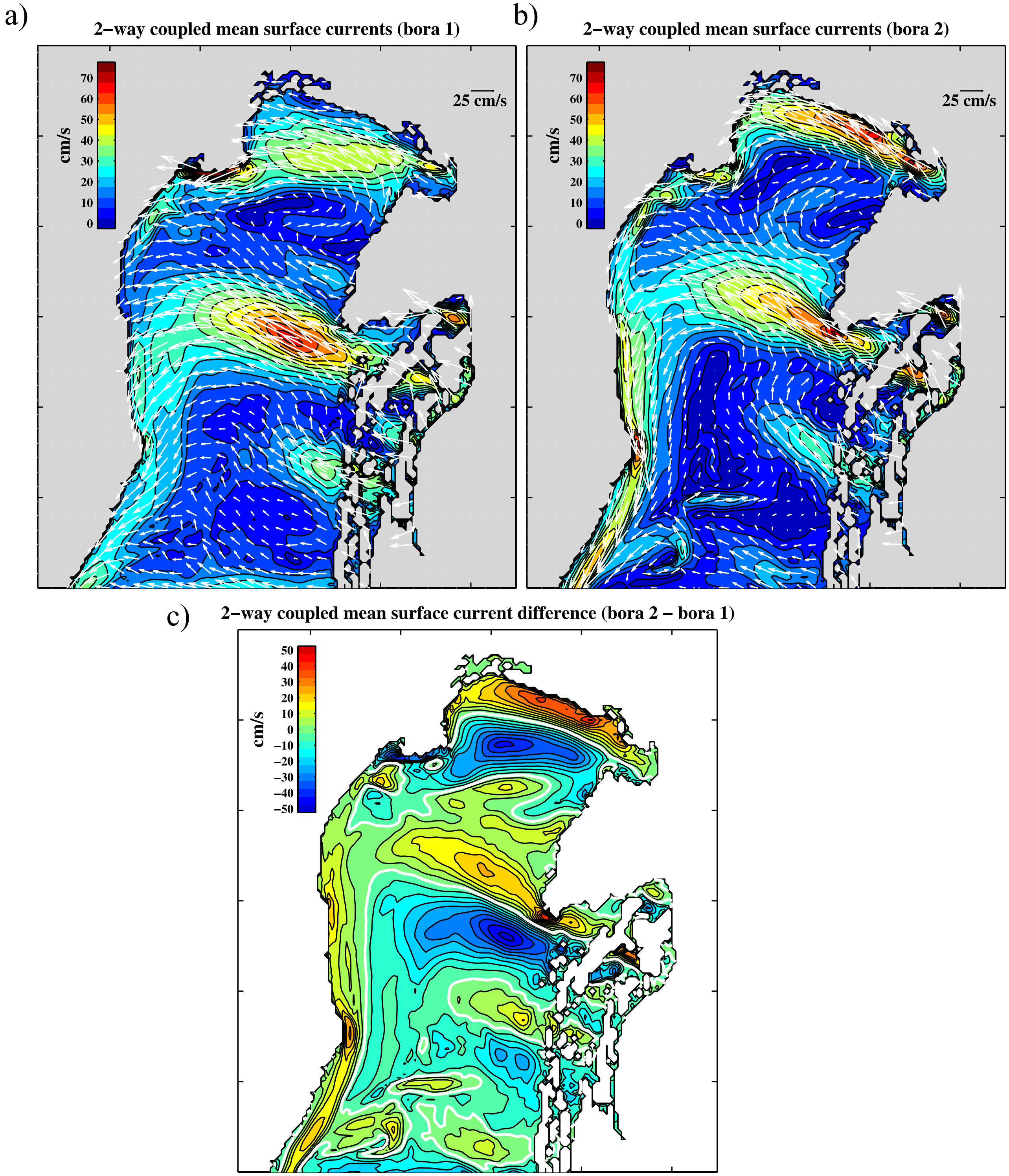

Figure 8. Mean two-way coupled ocean surface currents during bora 1 and 2, and surface current difference between bora 2 and 1.

with flood times (e.g., in early December 2002 the peak discharge was approximately 6000 m^3 s^{-1}). Instead, the WAC is presumably energized by the barrier jet that occurs at early morning times during bora 2 (see Figure 5c). Finally, in the central Adriatic south of the Senj jet, the flow is oriented east–west in bora 1 but north–south in bora 2.

[40] In order to evaluate the impact of the two-way coupled momentum and heat fluxes on modeled ocean circulation, a one-way coupled simulation is conducted. This one-way coupled run uses direct momentum fluxes from the control run to force the ocean model, while heat fluxes are recomputed using bulk formulae and the ocean model SST before they are applied to the ocean model, as

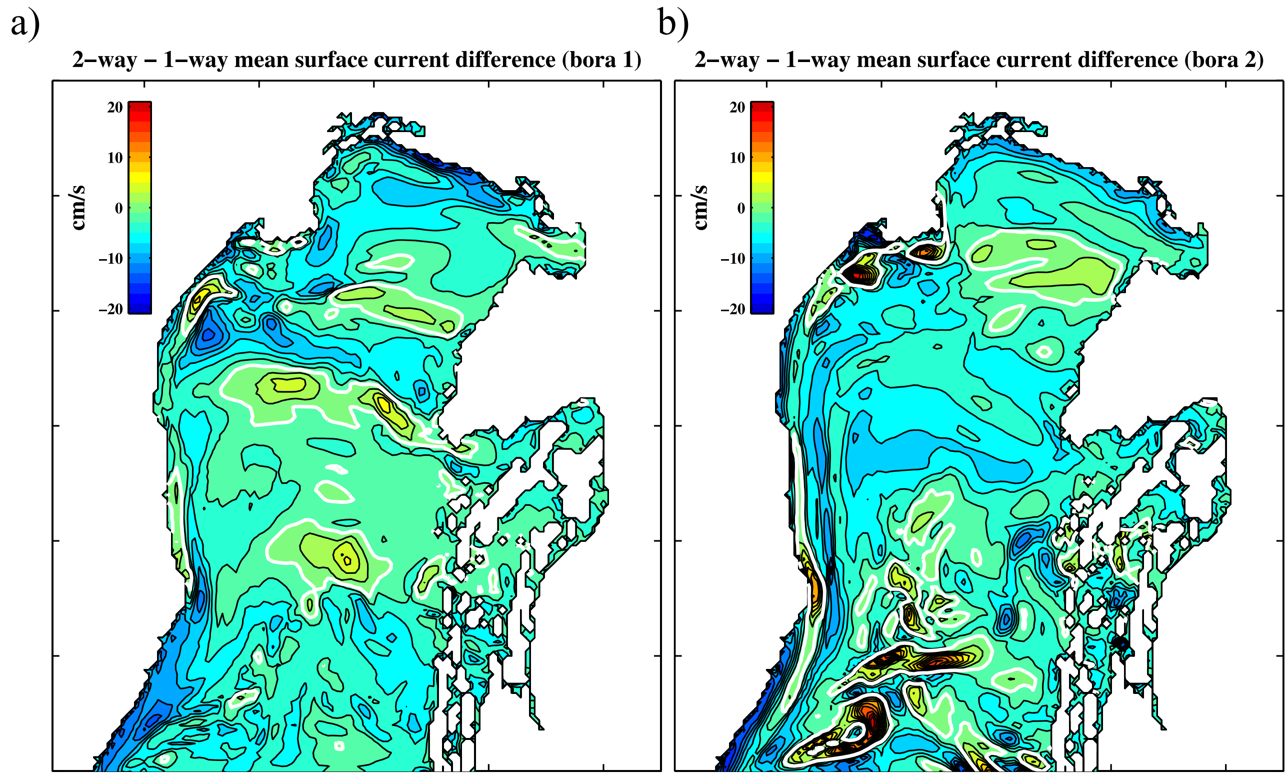

Figure 9. Two-way minus one-way coupled mean surface current difference for bora 1 and bora 2.

detailed in section 2. The intrabora comparison of the two-way and one-way coupled runs shows generally decreased mean surface current speed in the two-way coupled run during both bora (Figure 9). Despite small pockets of increased speed, the mean reduction in current speed over the area shown in the figure is 3 cm s^{-1} (11–12%) in both bora. The current speeds are reduced by over 10 cm s^{-1} in bora 1 and bora 2 in some regions. This is evident in the southern part of the WAC and along the northern edge of the Adriatic.

[41] Some of the regions of stronger current in the two-way coupled run are linked to differences in the wind stress curl fields between the simulations. For instance, swifter (by several cm s^{-1}) ocean flow that is oriented more onshore (vectors not shown) in the northern arm of the anticyclonic Rovinj gyre exists beneath the region of more negative curl in the two-way coupled simulation. Such correspondences are evident during both bora. Thus, the double gyre is a feature present in both bora (with some positional and magnitude differences), and the anticyclonic gyre is strengthened by two-way coupling.

6. Heat Flux Considerations

[42] Heat fluxes for the one-way coupled run were computed using the bulk flux algorithm applied to the control fields and ocean model SSTs [*Kondo*, 1975]. These fluxes were archived in order to evaluate whether the heat flux differences between the control and two-way coupled run could be ameliorated by creating heat fluxes that reflect both the air and ocean modeled temperatures. That is, can a better heat flux product (i.e., using ocean model SSTs instead of analyzed SSTs) be created that can replicate the improvements that were obtained using two-way coupling? This section does not supply a definitive answer as it only uses one bulk algorithm, but it does constitute an exploration of the topic. The pattern of one-way coupled heat fluxes mirrors those of the two-way coupled run during both bora (not shown). However, the one-way coupled mean heat fluxes are too strong in both bora. In bora 1, the one-way coupled simulation generates a mean domain-averaged total heat flux that is on average 77 W m^{-2} higher than in the two-way coupled simulation. In the bora jets the one-way coupled total heat flux exceeds the two-way coupled total heat flux by over 150 W m^{-2}. In bora 2 the total heat flux over the domain is 53 W m^{-2} greater in the one-way coupled simulation. As in bora 1, the jet areas display over 150 W m^{-2} stronger fluxes relative to the two-way coupled run.

[43] The one-way coupled simulation produces heat fluxes that are reduced relative to the control simulation, and thus more in accord with observed fields. However, there is twice as much reduction in heat flux in the two-way coupled run relative to the one-way coupled run. Therefore, the two-way coupled heat fluxes are smaller than both the control and one-way coupled fields and constitute a superior product considering the heat flux observations available in winter 2003 (as detailed in the next section).

7. Validation and Statistics

[44] There are important distinctions between the momentum and heat flux fields generated by the control and two-way coupled runs over the course of consecutive bora in winter 2003. These differences have a pronounced spatial pattern that is closely related to the SST field, which

Table 1. The 1–21 February 2003 Model Statistics at Individual Station Sites for Total Heat Flux (Positive Upward) and Wind Stress

	Control Mean, W m^{-2}	Two-Way Mean, W m^{-2}	Percent Reduction of Mean	Control Standard Deviation	Two-Way Standard Deviation	Percent Reduction of Standard Deviation
			Total Heat Flux (Positive Upward)			
Venice	263	162	38%	206	189	8%
Azalea	270	154	43%	180	163	9%
Ancona	290	78	73%	179	163	9%
Veli Rat	392	322	18%	259	232	10%
	Control Mean, N m^{-2}	Two-Way Mean, N m^{-2}	Percent Reduction of Mean	Control Standard Deviation	Two-Way Standard Deviation	Percent Reduction of Standard Deviation
			Wind Stress			
Venice	0.1647	0.1221	26%	0.1307	0.1172	10%
Azalea	0.1464	0.1023	30%	0.1030	0.0874	15%
Ancona	0.1245	0.0616	51%	0.0902	0.0690	24%
Veli Rat	0.1913	0.1349	30%	0.1561	0.1423	9%

was surveyed in section 4. Here we turn to a point comparison of wind stress and heat flux values for a longer period of time. Statistics of mean and standard deviation along with the percent reductions in the two-way coupled run relative to the control run are presented at four locations (marked in Figures 4 and 7) for 1–21 February 2003 (Table 1). At all four locations there is a reduction in wind stress and heat flux in the two-way coupled run compared with the control run. The greatest reduction in mean heat flux and wind stress (73% and 51%, respectively) occurs at Ancona. All locations have a comparable reduction in heat flux standard deviation of 8–10%, while Ancona had the greatest reduction in wind stress standard deviation (24%). Ancona is situated on the west side of the Adriatic where cooler SSTs are generated in the two-way coupled simulation.

[45] The smallest reduction of mean heat flux occurred at Veli Rat (18%), while the smallest reduction in wind stress occurred at Venice (26%). Minimal reduction in wind stress standard deviation was also found at Veli Rat (9%). Even though the percent change between the model runs is generally smallest at Veli Rat, the mean and standard deviation of heat flux and wind stress is greatest at that site in both models. Veli Rat is located on the edge of a bora jet and appears to be impacted by bora effects intermittently and occasionally powerfully (e.g., during bora 1 but not during bora 2 as shown in Figures 4 and 5).

[46] *Dorman et al.* [2006] reported on observations at the four stations, including details of the instrument suite. Here we compare the wind stress and heat flux observations with the model results. At Ancona, there were 36 latent and sensible heat flux hourly values missing throughout the 480 hour record (1–21 February 2003) used in the comparison. The longest consecutive gap was 6 hours. A spline interpolation was used to fill the gaps in the Ancona measurements. Also, the Azalea and Veli Rat sites began recording data on 9 February 2003, so the time series for comparison at those sites is truncated.

[47] At Ancona, the agreement with the observed fields is highly dependent on the coupling (Figure 10). There is quite striking correspondence between the two-way coupled latent and sensible heat fluxes, which translates into a skillful total heat flux model field. The two-way coupled simulation replicates well the diurnal total heat flux cycle, and generally captures the bora events in the wind stress record. The control run heat fluxes are too strong, especially during the high wind events on 1 and 5 February. Overall, the control run overestimates the observed wind stress field at Ancona.

[48] These qualitative assessments are made more concrete and extended to the other stations using basic and comparison statistics of heat flux (Table 2). The largest observed and modeled mean and standard deviation of heat flux occur at Veli Rat, even though that record began after 9 February and misses the major bora events early in the month that were contained in the statistics of Table 1. The weakest mean heat flux is at Azalea, which neither simulation captures. Weak midbasin heat fluxes were a characteristic of the observations noted by *Dorman et al.* [2006]. The smallest standard deviation of heat flux occurs at Ancona in the observed and model records. The control and two-way coupled mean biases are both largest at Azalea, but the two-way coupled run has a 44% reduced mean bias over the control run. The largest RMSE of the control and two-way coupled heat flux occurs at the Venice site. The two-way coupled simulation reduces the RMSE at Venice by 27%. Overall at all four stations, the mean bias is reduced by 72% in the two-way coupled simulation while the RMSE is reduced by 30% in the two-way coupled simulation. Correlation coefficients are slightly higher for the two-way coupled simulation compared with the control simulation.

[49] Basic and comparison statistics are also computed for wind stress (Table 3). The largest mean and fluctuating wind stress is found at Venice in the observational record and both models. The smallest observed mean and fluctuating wind stress is at Azalea. While both simulations have weakest fluctuations at Azalea, they differ from the observations by having the smallest mean wind stress at Ancona. The mean bias is reduced at all sites by the two-way coupled interaction. However, at Venice and Ancona the absolute mean bias is greater in the two-way coupled simulation, indicating too weak winds at Venice and Ancona in the two-way coupled simulation. The mean bias is largest at Azalea in both simulations, but that bias is reduced by 50% with two-way coupling. RMSEs are largest at Venice and smallest at Veli Rat in both simulations. There is a marked reduction of RMSE using two-way coupling at all sites save Venice. Correlation coefficients are slightly higher in the control simulation, except at Ancona.

8. Discussion and Conclusions

[50] Recent comparisons of over-water observations with winter 2003 control COAMPS 4-km resolution surface flux

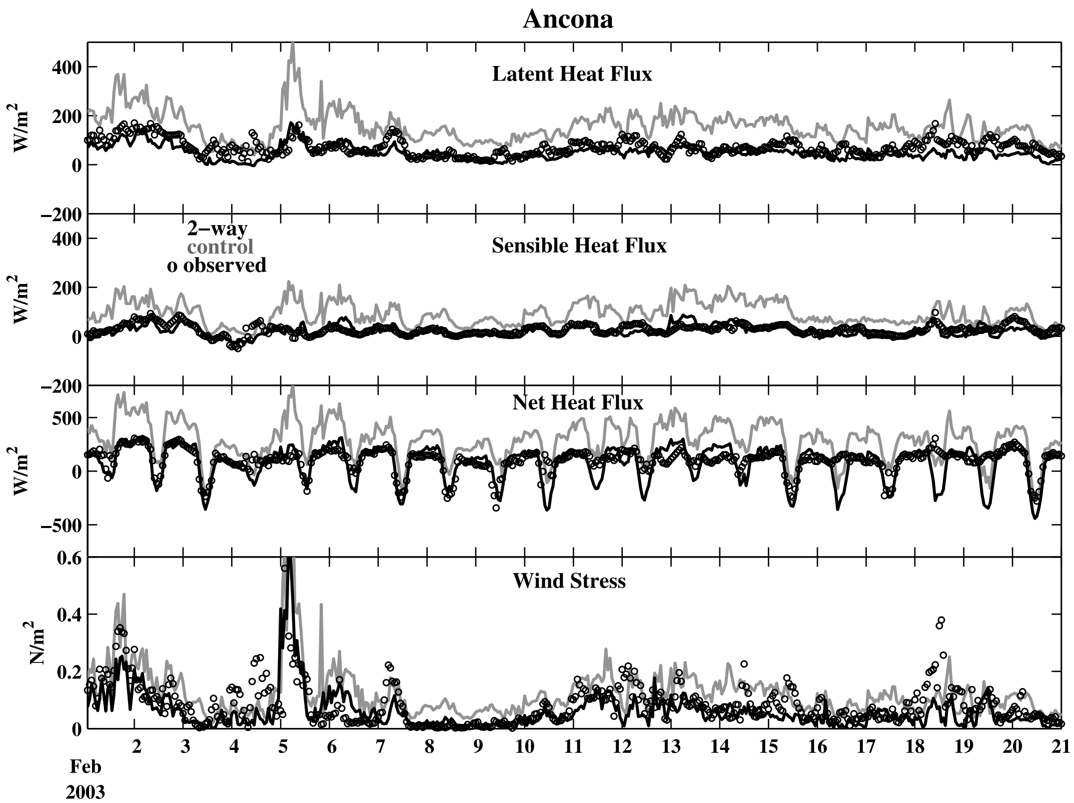

Figure 10. Time series of modeled (two-way coupled and control) and observed heat flux and wind stress at Ancona for 1–21 February 2003.

fields [*Dorman et al.*, 2006], and comparisons of in situ measurements of ocean velocity with modeled surface current fields forced by momentum fluxes from the control 4-km resolution COAMPS [*Kuzmic et al.*, 2006] reveal the modeled surface fluxes to be too strong in the northern Adriatic. The work presented in this paper set out to improve upon the surface fluxes in winter 2003. An additional goal of this work was to look at the differences in structure of the surface flux fields during two distinct consecutive bora events: one strong and one weak.

[51] Our approach was to employ two-way coupling of a meteorological model (COAMPS) with an ocean model (NCOM). Our prior work using this approach had resulted in reduced wind speeds in the two-way coupled run relative to a control run, with the two-way coupled run agreeing better with coastal and over-water wind measurements. However, *Pullen et al.* [2006] did not examine surface fluxes in detail in that work. Furthermore, these previous simulations were conducted for fall 2002. Fall is a transition season where the ocean is typically warmer and more stratified than it becomes later in the winter after the repeated experience of bora events. The ocean becomes well-mixed vertically and temperatures become more horizontally heterogeneous during winter. Thus we undertook to compare two-way coupled surface flux fields with over-water observations available in February 2003. We also embarked on an investigation of the variations at the interface of the ocean and atmosphere produced by two contrasting bora.

[52] In both the control and two-way coupled simulation, bora 1 (1400 UTC 31 January to 0600 UTC 2 February 2003) is stronger than bora 2 (0700 UTC 11 February to 0400 UTC 14 February 2003) in terms of mean total heat flux and wind stress in the jets and in the domain average. Bora 1 has a well-defined boundary layer and is warmer than bora 2. The synoptic setting of bora 2 introduces temporal displacements in the pressure gradient field that alter the positions of the jets so they do not steadily occupy one fixed location. In addition, local effects like inertial oscillations and a diurnal barrier jet play a strong role in the dynamics of this weaker bora. The position of the Trieste jet is displaced farther north in bora 2. The jets extend farther across the basin in bora 1, while bora 2 contains an episodic barrier jet along the west side of the Adriatic which hinders the extension of the Senj jet. In both simulations, bora 1 displays larger and more horizontally banded wind stress curl than bora 2.

[53] The atmospheric boundary layer interacts with spatially heterogeneous, and often cold, SSTs in the two-way coupled simulation, leading to overall reductions of mean total heat flux of (133 W m^{-2} or 23%) during bora 1 and (102 W m^{-2} or 26%) during bora 2 relative to the control simulation. The modified Louis scheme used in the two-way coupled run but not in the control run (described in section 2) can account for a portion of these differences, estimated to be less than half of the reduction seen in the bora jets. Outside the bora jets the reduction due to the modified surface flux scheme is much less. *Pullen et al.* [2006] utilized the modified Louis scheme in all simulations and documented appreciable differences in surface fluxes between the two-way and one-way coupled simulations.

Table 2. February 2003 Modeled and Observed Statistics for Total Heat Flux at Individual Station Sites: Basic Statistics and Comparison Statistics[a]

W m^{-2}	N	Mean	Standard Deviation
Basic Statistics			
Venice			
Obs	480	62	190
Control	480	263	206
Two-way	480	162	189
Azalea			
Obs	288	15	165
Control	288	264	183
Two-way	288	156	166
Ancona			
Obs	480	101	112
Control	480	290	179
Two-way	480	78	163
Veli Rat			
Obs	276	280	296
Control	276	360	248
Two-way	276	296	229
W m^{-2}	MB	RMSE	CC
Comparison Statistics			
Venice			
Control	−202	275	0.55
Two-way	−100	202	0.57
Azalea			
Control	−248	215	0.75
Two-way	−140	139	0.77
Ancona			
Control	−189	229	0.69
Two-way	23	119	0.70
Veli Rat			
Control	−80	169	0.72
Two-way	−16	155	0.73

[a]MB, mean bias; RMSE, root mean square error; CC, correlation coefficient.

Total heat flux standard deviation, along with wind stress mean, standard deviation, and curl are likewise diminished in the two-way coupled simulation. The latter two quantities present strong sensitivity to the Istrian front location between the control and two-way coupled simulations during bora 1. Generally, the largest absolute reductions of surface fluxes occur during bora 1 (the stronger bora) and the greatest percent reductions occur during bora 2. Coupling is a factor in the SST-induced reduction of wind stress curl in the Trieste jet along the northern coast during bora 2, and in the diminished wind stress and wind stress curl under the barrier jet that overlies cold SSTs along the western side of the Adriatic.

[54] Differences in bora surface flux structure lead to differences in ocean surface currents in the two-way coupled simulation. Whereas in bora 1 the current is stronger in the westward flow near the Istrian Peninsula tip, in bora 2 the current is stronger in the northern arm of the Trieste gyre and the WAC. The strengthened Trieste gyre flow of bora 2 can be linked to the stronger positive wind stress curl found in the Gulf of Trieste during bora 2. The strengthened westward flow south of the Istrian Peninsula in bora 1 may be linked to larger positive wind stress curl south of the Istrian Peninsula at that time. The energized WAC flow during bora 2 is likely associated with the intermittent atmospheric barrier jet.

[55] Modeled ocean currents forced by the control momentum fluxes were too strong when compared with ADCP observations [*Kuzmic et al.*, 2006]. The two-way coupled simulation produces current speeds reduced by 11–12% (~3 cm s^{-1}) during both bora relative to one-way coupled speeds. In the WAC and along the north coast differences exceed 10 cm s^{-1} in some locations during both bora. Localized areas of stronger currents in the two-way coupled simulation occur under regions of stronger negative wind stress curl in both bora compared with the one-way coupled simulation. This produces a stronger anticyclonic Rovinj gyre in the two-way coupled simulation.

[56] Improvements in the total heat flux are attained using a bulk flux algorithm [*Kondo*, 1975] that incorporates air and ocean model temperatures. However, the total heat fluxes are still too strong relative to the two-way coupled run (by on average 77 W m^{-2} in bora 1 and 53 W m^{-2} in bora 2). Recent investigations applying bulk flux formulations to different observational data sets suggest that utilizing the new COARE 3.0 algorithm [*Fairall et al.*, 2003] may improve bulk flux-derived heat and momentum fluxes [*Brunke et al.*, 2003]. Such a comparative study is underway for the Adriatic data set (R. P. Signell et al., manuscript in preparation, 2006), but this would not ameliorate the value of two-way coupling in improving atmospheric forecasts of boundary layer quantities.

[57] In comparisons with observations at four over-water sites in the northern Adriatic, the control and two-way coupled surface fluxes matched the spatial pattern of strongest mean and fluctuations (Veli Rat for heat flux and Venice for momentum flux) at these sites scattered across the basin. Though both simulations accurately pinpoint the site of weakest fluctuations (Ancona for heat and Azalea for momentum), neither simulation pegged the location of weakest mean fluxes (Azalea). The greatest mean bias in

Table 3. As in Table 2, but for Wind Stress

N m^{-2}	N	Mean	Standard Deviation
Basic Statistics			
Venice			
Obs	480	0.1507	0.1676
Control	480	0.1647	0.1307
Two-way	480	0.1221	0.1172
Azalea			
Obs	288	0.0632	0.0572
Control	288	0.1436	0.0802
Two-way	288	0.1017	0.0691
Ancona			
Obs	480	0.0852	0.0754
Control	480	0.1245	0.0902
Two-way	480	0.0616	0.0690
Veli Rat			
Obs	276	0.0923	0.0703
Control	276	0.1602	0.0988
Two-way	276	0.1038	0.0821
N m^{-2}	MB	RMSE	CC
Comparison Statistics			
Venice			
Control	−0.0140	0.1238	0.68
Two-way	0.0286	0.1320	0.64
Azalea			
Control	−0.0804	0.0828	0.52
Two-way	−0.0385	0.0593	0.46
Ancona			
Control	−0.0393	0.0879	0.56
Two-way	0.0237	0.0698	0.59
Veli Rat			
Control	−0.0679	0.0734	0.71
Two-way	−0.0115	0.0469	0.69

heat and momentum flux is at Azalea, and was reduced by 44% and 50%, respectively, using two-way coupling.

[58] Structural distinctions between bora have long been noted in the meteorological literature [*Defant*, 1951]. However, most previous ocean model simulations utilized idealized atmospheric winds [*Orlic et al.*, 1994; *Paklar et al.*, 2005] or simulated only one bora event [*Paklar et al.*, 2001]. By contrast the simulations presented here are focused on differentiating the ocean and atmosphere response during two distinct bora. Notable differences between the patterns of surface fluxes and circulation in the ocean and atmosphere were found during this study, challenging the notion of a "typical" bora. In addition, the inclusion of two-way coupled ocean-atmosphere coupling enabled more realistic surface fluxes to be attained for February 2003 that agreed better with measurements and resulted in reduced ocean surface current speeds during the bora events that were more consistent with observations.

[59] In addition, SST-induced effects on wind stress curl were evident in the barrier jet and Trieste jet of the two-way coupled simulation. Such wind stress curl modifications impacted the two-way coupled ocean currents by intensifying the Rovinj gyre. These effects occurring on very small scales in this realistic simulation augment other studies documenting the impact of SST gradients on wind stress curl over the global ocean [*Chelton et al.*, 2004].

[60] The SST feedback in the two-way coupling occurred at a 6-hour interval in our numerical experiment. This coupling timescale was sufficient to capture the major trends in SST variability, but may have missed short-duration feedback effects. We are currently testing the sensitivity of the coupled response to the feedback interval. Also of note is the advent of high-resolution SST fields from increasingly sophisticated remote-sensing platforms. Though this will lead to more accurate representation of SST gradients in analyzed SST fields, it still cannot compensate for the predictive skill supplied by a coupled forecast model [*Pullen et al.*, 2006]. More sensitivity studies are needed to carefully isolate the impacts of high-resolution SSTs from the impacts due to the coupled response.

[61] **Acknowledgments.** We gratefully acknowledge Luigi Cavaleri for supplying the Acqua Alta tower data. We wish to thank Courtney Harris and Aaron Bever for organizing the river discharge data. Thanks to Ivica Janekovic for drafting an original version of Figure 1. The hospitality of the NATO Undersea Research Centre was instrumental in facilitating the collaboration of the authors. Computations were conducted under the DoD Major Shared Research Center High Performance Computing Challenge Program on SGI Origin 3000s at ARL (Aberdeen, Maryland) and ERDC (Vicksburg, Mississippi). The research support for J. Pullen, J. D. Doyle, and T. Haack was provided by the Office of Naval Research (ONR) program elements 0602435N and 0601153N.

References

Brunke, M. A., C. W. Fairall, X. Zeng, L. Eymard, and J. A. Curry (2003), Which bulk aerodynamic algorithms are least problematic in computing ocean surface turbulent fluxes?, *J. Clim.*, *16*, 619–635.

Chelton, D. B., M. G. Schlax, M. F. Freilich, and R. F. Milliff (2004), Satellite measurements reveal persistent small-scale features in ocean winds, *Science*, *303*, 978–983.

Chen, S., et al. (2003), COAMPS™ Version 3 Model Description, 143 pp., Mar. Meteorol. Div., Nav. Res. Lab., Monterey, Calif.

Defant, F. (1951), Local winds, in *Compendium of Meteorology*, edited by T. F. Malone, pp. 655–672, Am. Meteorol. Soc., Boston, Mass.

Dorman, C. E., et al. (2006), February 2003 marine atmospheric conditions and the bora over the northern Adriatic, *J. Geophys. Res.*, *111*, C03S03, doi:10.1029/2005JC003134. [printed *112*(C3), 2007]

Enger, L., and B. Grisogono (1998), The response of bora-type flow to sea surface temperature, *Q. J. R. Meteorol. Soc.*, *124*, 1227–1244.

Fairall, C. W., E. F. Bradley, J. E. Hare, A. A. Grachev, and J. B. Edson (2003), Bulk parameterization of air-sea fluxes: updates and verification for the COARE algorithm, *J. Clim.*, *16*, 571–591.

Garratt, J. R. (1985), Inland boundary layer at low latitudes. Part 1, the nocturnal jet, *Boundary Layer Meteorol.*, *32*, 307–327.

Gohm, A., and G. J. Mayr (2005), Numerical and observational case-study of a deep Adriatic bora, *Q. J. R. Meteorol. Soc.*, *131*, 1363–1392.

Grubisic, V. (2004), Bora-driven potential vorticity banners over the Adriatic, *Q. J. R. Meteorol. Soc.*, *130*, 2571–2603.

Hodur, R. M. (1997), The Naval Research Laboratory's Coupled Ocean/Atmosphere Mesoscale Prediction System (COAMPS), *Mon. Weather Rev.*, *125*, 1414–1430.

Jiang, Q., and J. D. Doyle (2005), Wave breaking induced surface wakes and jets observed during a bora event, *Geophys. Res. Lett.*, *32*, L17807, doi:10.1029/2005GL022398.

Jurcec, V. (1988), The Adriatic frontal bora type, *Croatian Meteorol.*, *23*, 13–25.

Jurcec, V. (1989), Severe Adriatic bora storms in relation to synoptic developments, *Meteorology*, *24*, 11–20.

Kondo, J. (1975), Air-sea bulk transfer coefficients in diabatic conditions, *Boundary Layer Meteorol.*, *9*, 91–112.

Kraus, H., J. Malcher, and E. Schaller (1985), Nocturnal low-level jet during PUKK, *Boundary Layer Meteorol.*, *31*, 187–195.

Kuzmic, M., I. Janekovic, J. W. Book, P. J. Martin, and J. D. Doyle (2006), Modeling the northern Adriatic double-gyre response to intense bora wind: A revisit, *J. Geophys. Res.*, *111*, C03S13, doi:10.1029/2005JC003377. [printed *112*(C3), 2007]

Lee, C., et al. (2005), Northern Adriatic response to a wintertime bora wind event, *Eos Trans. AGU*, *86*(16), 157, 163, 165.

Louis, J. F., M. Tiedtke, and J. F. Geleyn (1981), A short history of the operational PBL parameterization at ECMWF, in *Proceedings of Workshop on Boundary Layer Parameterizations*, pp. 59–80, Eur. Cent. for Medium-Range Weather Forecasts, Reading, U.K.

Martin, P. J. (2000), A description of the Navy Coastal Ocean Model version 1.0, *Nav. Res. Lab. Rep. NRL/FR/7322-00-9962*, 42 pp., Nav. Res. Lab., Stennis Space Cent., Miss.

Martin, P. J., J. W. Book, and J. D. Doyle (2006), Simulation of the northern Adriatic circulation during winter 2003, *J. Geophys. Res.*, *111*, C03S12, doi:10.1029/2006JC003511. [printed *112*(C3), 2007]

Orlic, M., M. Kuzmic, and Z. Pasaric (1994), Response of the Adriatic Sea to the bora and sirocco forcing, *Cont. Shelf Res.*, *14*, 91–116.

Paklar, G. B., V. Isakov, D. Koracin, V. Kourafalou, and M. Orlic (2001), A case study of bora-driven flow and density changes on the Adriatic Shelf (January 1987), *Cont. Shelf Res.*, *21*, 1751–1783.

Paklar, G. B., A. Bajic, V. Dadic, B. Grbec, and M. Orlic (2005), Bora-induced currents corresponding to different synoptic conditions above the Adriatic, *Ann. Geophys.*, *23*, 1083–1091.

Peters, H., C. M. Lee, M. Orlic, and C. E. Dorman (2006), Turbulence in the wintertime northern Adriatic Sea under strong atmospheric forcing, *J. Geophys. Res.*, doi:10.1029/2006JC003634, in press.

Pullen, J., J. D. Doyle, R. Hodur, A. Ogston, J. W. Book, H. Perkins, and R. Signell (2003), Coupled ocean-atmosphere nested modeling of the Adriatic Sea during winter and spring 2001, *J. Geophys. Res.*, *108*(C10), 3320, doi:10.1029/2003JC001780.

Pullen, J., J. D. Doyle, and R. Signell (2006), Two-way air-sea coupling: a study of the Adriatic, *Mon. Weather Rev.*, *134*(5), 1465–1483.

Raicich, F. (1994), Note on the flow rates of the Adriatic rivers, *Tech. Rep. RF 02/94*, 8 pp., CNR Istituto Sperimentale Talassografico, Trieste, Italy.

Sherwood, C., et al. (2004), Sediment dynamics in the Adriatic Sea investigated with coupled models, *Oceanography*, *17*(4).

Smith, R. B. (1987), Aerial observations of the Yugoslavian bora, *J. Atmos. Sci.*, *44*, 269–297.

Wang, S., Q. Wang, and J. Doyle (2002), Some improvement of Louis surface flux parameterization, paper presented at 15th Symposium on Boundary Layers and Turbulence, Am. Meteorol. Soc., Wageningen, Netherlands.

Zore-Armanda, M., and M. Gacic (1987), Effects of bora on the circulation in the Northern Adriatic, *Ann. Geophys., Ser. B*, *5*, 93–102.

C. Dorman, Scripps Institution of Oceanography, University of California, San Diego, La Jolla, CA 92093-0209, USA.

J. D. Doyle, T. Haack, and J. Pullen, Marine Meteorology Division, Naval Research Laboratory, 7 Grace Hopper Avenue, Monterey, CA 93943, USA. (julie.pullen@nrlmry.navy.mil)

C. M. Lee, Applied Physics Laboratory, University of Washington, Seattle, WA 98105-6698, USA.

R. P. Signell, U.S. Geological Survey, Woods Hole, MA 02543, USA.